Roles of Armadillo, a *Drosophila* catenin, during central nervous system development

Joseph Loureiro* and Mark Peifer*†

Background: Neural development requires that neurons communicate and co-operate with one another and with other cell types in their environment. *Drosophila* Armadillo and its vertebrate homolog β-catenin have dual roles in epithelial cells: transducing signals from the Wingless/Wnt family of proteins and working with cadherins to mediate cell adhesion. Wingless/Wnt signaling also directs certain cell fates in the central nervous system (CNS), and cadherins and catenins are thought to function together during neural development.

Results: We identified and analyzed the biochemical properties of a second *armadillo* isoform, with a truncated carboxyl terminus generated by alternative splicing. This isoform was found to accumulate in differentiating neurons. Using *armadillo* alleles that selectively inactivate the cell adhesion or the Wingless signaling functions of Armadillo, we found that Armadillo had two sequential roles in neural development. Armadillo function in Wingless signal transduction was required early in development for determination of neuroblast fate. Later in development, disruption of the cell–cell adhesion function of Armadillo resulted in subtle defects in the construction of the axonal scaffold. Mutations in the gene encoding the *Drosophila* tyrosine kinase Abelson substantially enhanced the severity of the CNS phenotype of *armadillo* mutations, consistent with these proteins functioning co-operatively at adherens junctions in both the CNS and the epidermis.

Conclusions: This is one of the first demonstrations of a role for the cadherin–catenin system in the normal development of the CNS. The genetic interactions between *armadillo* and *abelson* point to a possible role for the tyrosine kinase Abelson in cell–cell adhesive junctions in both the CNS and the epidermis.

Addresses: *Department of Biology and †Curriculum in Genetics and Molecular Biology, University of North Carolina, Chapel Hill, North Carolina 27599-3280, USA.

Correspondence: Mark Peifer
E-mail: peifer@unc.edu

Received: 22 January 1998
Revised: 7 April 1998
Accepted: 7 April 1998

Published: 6 May 1998

Current Biology 1998, 8:622–632
http://biomednet.com/elecref/0960982200800622

Background

Drosophila Armadillo (Arm) and its vertebrate homolog β-catenin have dual roles in epithelial tissues, transducing signals from the Wingless/Wnt family of proteins and mediating cadherin-based intercellular adhesion (reviewed in [1]). Wingless/Wnts, cadherins and catenins also accumulate in the nervous system, where they presumably have biochemical roles similar to those in epithelia. Here, we have expanded our previous analysis of the roles of these proteins in the epidermis and examined their possible roles in the central nervous system (CNS).

Embryonic development of the *Drosophila* CNS passes through distinct phases. First, segmentally reiterated sets of neuroblasts acquire positional identities by integrating their intrinsic program of development with signals from other neuroblasts. The Wingless (Wg) signal directs specific neuroblast identities [2]. In the epidermis, Wg also directs cell fates, and Arm is essential for Wg signal transduction (reviewed in [1]). Subsequently, neuroblast descendants differentiate as post-mitotic neurons, projecting axons toward specific targets in response to environmental cues. A diverse array of transmembrane glycoproteins, such as cadherins and fasciclins, are thought to guide axons, directing axon outgrowth and also mediating fasciculation, by which axon subsets selectively adhere to each other.

Cadherins, in conjunction with intracellular catenins, mediate homophilic cell–cell interactions. Within epithelia, cadherin–catenin complexes form the core of adherens junctions, mediating cell adhesion and anchoring the actin cytoskeleton. Arm connects *Drosophila* α-catenin to *Drosophila* E-cadherin [3]; this tripartite complex mediates adherens junction function [4,5]. Vertebrate N-cadherin accumulates in neurons, and in tissue culture it promotes polarized cellular outgrowth [6]. Antibody inhibition and dominant-negative experiments suggest that vertebrate N-cadherin mediates axon outgrowth, fasciculation and target recognition *in vivo* [7,8]. In the *Drosophila* CNS, axons accumulate both *Drosophila* N-cadherin [9] and Arm.

Both axon outgrowth and cell–cell adhesion may be modulated by tyrosine kinases and phosphatases. Membrane-associated non-receptor tyrosine kinases, including

Drosophila Abelson (Abl) and Dsrc41, localize to fly cell–cell junctions *in vivo* [10,11]; mammalian Abl also localizes to adherens junctions (F. Gertler, personal communication). Tyrosine kinases and phosphatases are thought to regulate assembly and disassembly of adherens junctions. One target may be Arm, which is phosphorylated on tyrosine, serine and threonine residues [12]. *Drosophila* Abl also has a role in axonogenesis. Although *abl* mutant animals have a normal CNS, embryos that are double mutant for *abl* and certain other genes have defects in axon outgrowth (reviewed in [13]). Abl may steer axonogenesis by regulating the actin cytoskeleton.

Results

A novel 82 kDa Arm isoform is produced by alternative splicing

Arm was found ubiquitously in embryos, with highest levels in the CNS. Arm was found both in neural cell bodies and, at significantly higher levels, in axons of the embryonic and larval (see below), and presumably adult, CNS. Antisera directed against Arm recognize differentially phosphorylated Arm isoforms of 105–115 kDa [12]. In addition, two polyclonal and three monoclonal anti-Arm antibodies (Figure 1a and data not shown) reacted with an 82 kDa protein; it thus seemed likely that the 82 kDa protein was a product of *arm*. However, neither monoclonal nor polyclonal antibodies directed against the carboxyl terminus of Arm cross-reacted with the 82 kDa protein (Figure 1e), suggesting that it differed from Arm at the carboxyl terminus. During embryogenesis, the 82 kDa protein was first seen after germ-band retraction as neurons began to differentiate (Figure 1a). In third instar larval brains that were carefully dissected to remove imaginal discs, the 82 kDa protein was the predominant protein reacting with the anti-Arm antibody (Figure 1b), suggesting that it was enriched in the CNS.

The 82 kDa protein was abundant in the adult head (data not shown). We thus isolated *arm* cDNAs from an adult head cDNA library and screened them by PCR for alternative splicing, using primer sets spanning two-thirds of the coding region. We identified two classes of cDNAs: 7 of 13 were identical to the original *arm* cDNAs whereas the remaining 6 were approximately 100 bp shorter, because of the absence of exon 6. One cDNA from the shorter class of cDNAs was completely sequenced. The only other differences from canonical *arm* were two silent nucleotide polymorphisms. We confirmed the presence of the shorter *arm* mRNA *in vivo* by reverse transcription (RT)–PCR. In 0–8 hour old embryos, in which the ubiquitous Arm isoform alone was detected by immunoblotting, only the longer mRNA was expressed, whereas in 14–20 hour old embryos, which contain both ubiquitous Arm and the 82 kDa isoform, both types of mRNA were found to be expressed (Figure 1d).

Figure 1

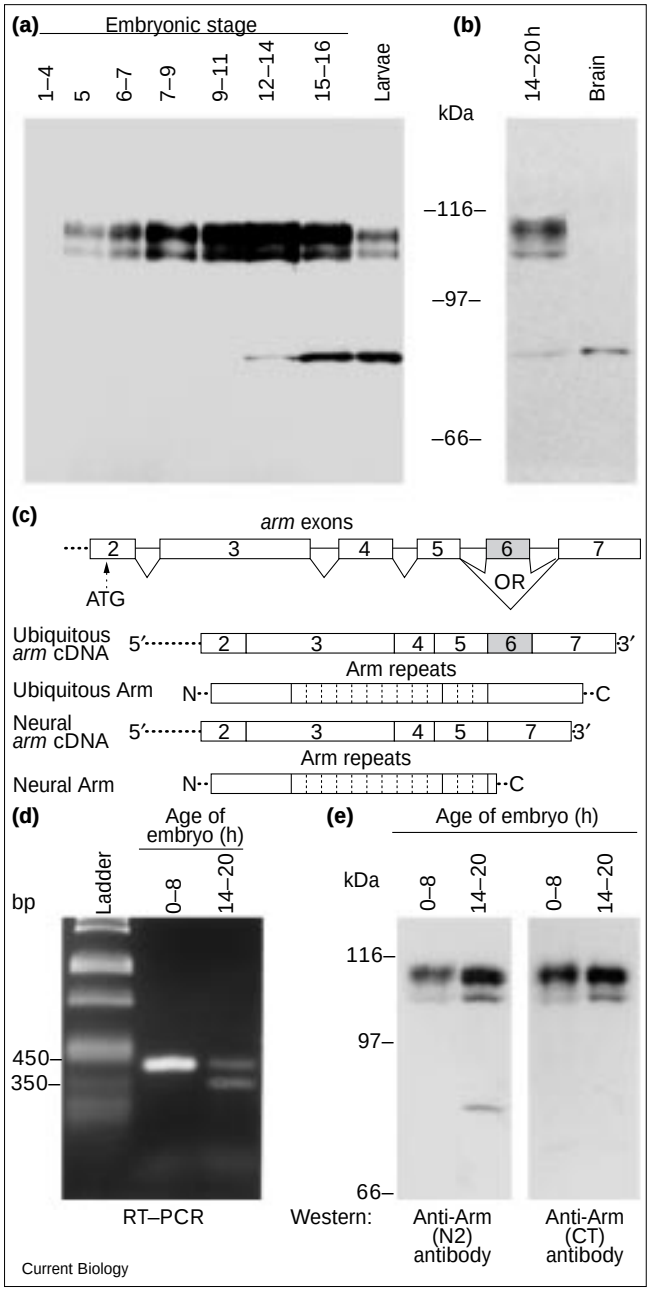

Identification of a CNS-enriched isoform of Arm. (a) Protein extracts from the indicated embryonic stages and from larvae immunoblotted with anti-Arm(N2) antibody. The 82 kDa protein first appeared after germ-band retraction during stage 12. (b) The 82 kDa protein was found to be enriched in the CNS. Late embryos (14–20 h post-fertilization) contained both ubiquitous Arm and the 82 kDa protein, whereas the 82 kDa protein accumulated preferentially in third instar larval brains. (c) Adult heads were found to contain two classes of *arm* transcripts. One encodes ubiquitous Arm and the other the 82 kDa Arm. N, amino terminus; C, carboxyl terminus; OR, alternatively spliced exon. (d) RT–PCR analysis using primers flanking exon 6 distinguished the two transcripts. Whereas the ubiquitous transcript was present throughout development, the shorter transcript was only detected in late embryos. (e) The 82 kDa isoform in late embryos was not detected with the anti-Arm(CT) antibody.

Thus the 82 kDa isoform is encoded by an alternative splice product of *arm*, with exon 5 spliced to exon 7, frame-shifting it such that a stop codon is introduced after only six codons into exon 7 (Figure 1c). Instead of encoding the ubiquitous 843 amino-acid polypeptide (91 kDa), the shorter transcript encodes a 721 amino-acid product (79 kDa) retaining the amino terminus and Arm repeat domains, which are required for catenin function, but with a truncated carboxyl terminus. Thus, the 82 kDa isoform cross-reacted with antibodies against the ubiquitous isoform that recognized the amino terminus, but not those that recognize the carboxyl terminus (Figure 1e).

The 82 kDa Arm isoform is neural Arm

We further tested whether the 82 kDa Arm isoform was enriched in the CNS by analyzing accumulation of the two Arm isoforms *in situ*. As the 82 kDa isoform differs from ubiquitous Arm by what it lacks, we adopted an indirect approach. Antibodies directed against the amino terminus of Arm, anti-Arm(N2), detected both the ubiquitous and 82 kDa isoforms whereas antibodies directed against the carboxyl terminus of ubiquitous Arm, anti-Arm(CT), recognized only the ubiquitous isoform. We thus double-labeled embryos, detecting anti-Arm(N2) labeling with rhodamine (red), and anti-Arm(CT) labeling with fluorescein (green). Tissues in which ubiquitous Arm accumulated appeared yellow, indicating co-localization of anti-Arm(N2) and anti-Arm(CT) labeling, whereas tissues that accumulated the 82 kDa protein predominantly appeared red, as that isoform only reacted with anti-Arm(N2) antibody.

From the cellular blastoderm stage until germ-band retraction, ubiquitous Arm was the predominant isoform (Figure 2a–d), consistent with the immunoblot data (Figure 1a). The 82 kDa isoform appeared after germ-band retraction initiated and accumulated in the developing longitudinal and commissural axon tracts of the CNS (Figure 2f–l). In contrast, ubiquitous Arm (recognized by the anti-Arm(CT) antibody) accumulated only to low levels in axons, but to high levels in specific cells along the CNS midline near each commissure (presumably midline glial cells; Figure 2g,h). As a control for differential labeling, we forced expression of ubiquitous Arm in the CNS using a prespliced *arm* transgene crossed into an *arm* null. These embryos expressed ubiquitous Arm in the CNS (Figure 2m). We henceforth refer to the 82 kDa isoform as neural Arm.

Neural Arm also accumulated in motor neurons of the segmental and intersegmental nerves as they exit the CNS (data not shown); it is difficult to assess which isoform these nerves accumulate once they become juxtaposed to tracheae expressing ubiquitous Arm. Both isoforms accumulated in the peripheral nervous system (Figure 2n,o). Neural Arm was detected in neural cell clusters such as chordotonal organs, whereas ubiquitous Arm had an intense but punctate localization at cell–cell junctions of peripheral sensory structures (these junctions are described in [14]). Leg and eye imaginal discs (including developing photoreceptors) accumulated ubiquitous Arm (Figure 2p,q). In the larval CNS, neural Arm accumulated along axon tracts, whereas ubiquitous Arm was enriched along the midline (Figure 2r). Thus, at all stages examined, neural Arm was the predominant isoform in axons whereas ubiquitous Arm was found in cell bodies and other specific structures.

Figure 2

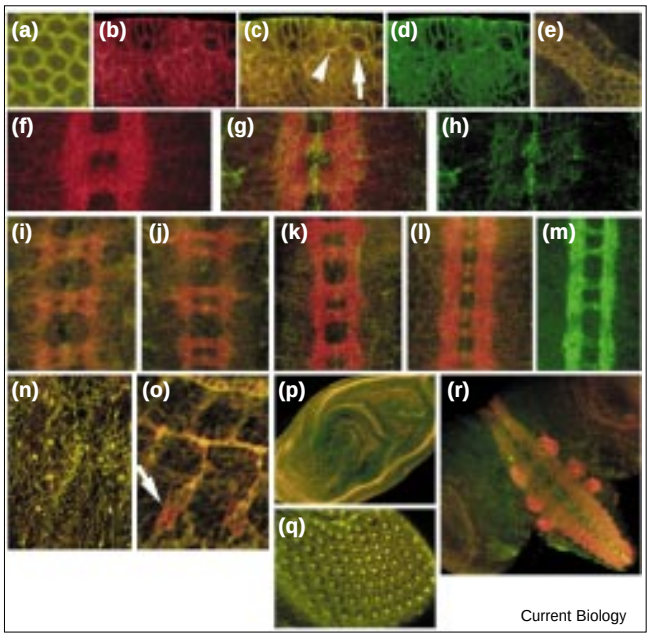

The 82 kDa Arm isoform is neural Arm. (a–o) Embryos or (p–r) third-instar larvae were double-labeled with anti-Arm(N2) antibody (red), which detects both ubiquitous and neural Arm, and anti-Arm(CT) antibody (green), which detects only ubiquitous Arm. In (a,c,e,g, i–l, n–r), the signals have been superimposed: yellow suggests predominance of ubiquitous Arm whereas red reveals predominance of neural Arm. (b,f) Anti-Arm(N2) signal. (d,h,m) Anti-Arm(CT) signal. (a–e) Ubiquitous Arm predominated in (a) embryos completing cellularization, (b–d) stage 9 embryos undergoing Wg signaling, and (e) stage 13 hindgut. (c) In segmentally repeated subsets of epidermal, neural and mesodermal cells, Arm accumulated in the cytoplasm and nucleus (arrowhead), but not in their neighbors (arrow). (f–h) A CNS segment from a stage 15 embryo. The anti-Arm(N2) antibody strongly labeled the CNS. The anti-Arm(CT) antibody labeled axons only faintly, but strongly labeled the ventral midline near each commissure. (i–l) Embryos from stages 13, 14, 15 and 16, respectively. Neural Arm accumulated in axons as they developed into the embryonic CNS. (m) In a transgenic embryo expressing ubiquitous Arm in axons, ubiquitous Arm accumulates in the CNS. (n,o) Both Arm isoforms accumulated in the peripheral nervous system. (n) In external sense organs, ubiquitous Arm accumulated in sensory sockets (lateral view of two segments shown). (o) Neural Arm was detected at chordotonal organ clusters (arrow). (p–r) Third instar larval leg imaginal disc (p), eye imaginal disc (q) and brain (r). Ubiquitous Arm was the predominant isoform in imaginal discs (p,q). In the larval brain (r), neural Arm accumulated in axons and ubiquitous Arm along the midline.

Figure 3

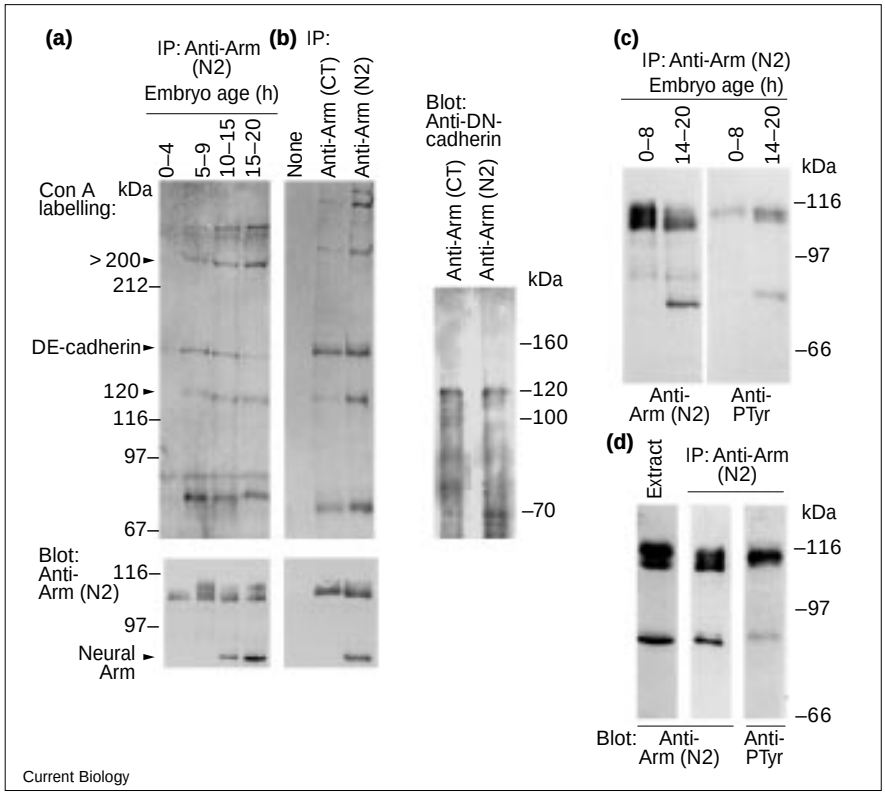

Biochemical characterization of neural Arm. (a) Immunoprecipitations using anti-Arm(N2) antibody on lysates derived from embryos of the indicated ages. Neural Arm was detected only in 10–20 h old embryos; lysates from these embryos were also enriched for certain glycoproteins, including one of 120 kDa. The approximately 150 kDa glycoprotein is DE-cadherin. (b) Anti-Arm(CT) antibody precipitated ubiquitous Arm but not neural Arm. Anti-Arm(CT) IPs were enriched for DE-cadherin in comparison with the 120 kDa and > 200 kDa glycoproteins. In contrast, nearly equal amounts of the 120 kDa and > 200 kDa glycoproteins and DE-cadherin were immunoprecipitated with the anti-Arm(N2) antibody, which recognizes both Arm isoforms. 'None' indicates Protein A–Sepharose alone. Similar IPs immunoblotted with anti-DN-cadherin antibody revealed that DN-cadherin was present in both IPs. (c) Anti-Arm(N2) antibody IPs were immunoblotted with anti-phosphotyrosine antibody (anti-PTyr), revealing a tyrosine-phosphorylated band migrating slightly more slowly than the 82 kDa isoform in late-stage embryos. (d) Anti-Arm(N2) antibody detected this same protein, which accumulated at lower levels than the unphosphorylated 82 kDa isoform.

Biochemical properties of the neural isoform

We found previously that a substantial fraction of both neural Arm and ubiquitous Arm is retained on concanavalin A (con A)–Sepharose [3,15] by virtue of association with a glycoprotein, presumably a cadherin. We thus examined the glycoproteins with which neural Arm interacts. An approximately 150 kDa glycoprotein, now known to be DE-cadherin [5,16], co-immunoprecipitates with ubiquitous Arm [15]. Labeling of anti-Arm immunoprecipitates (IPs) with con A also revealed glycoproteins of 120 kDa and > 200 kDa (Figure 3a,b); differential immunoprecipitation with different anti-Arm antibodies and coincidence of

Figure 4

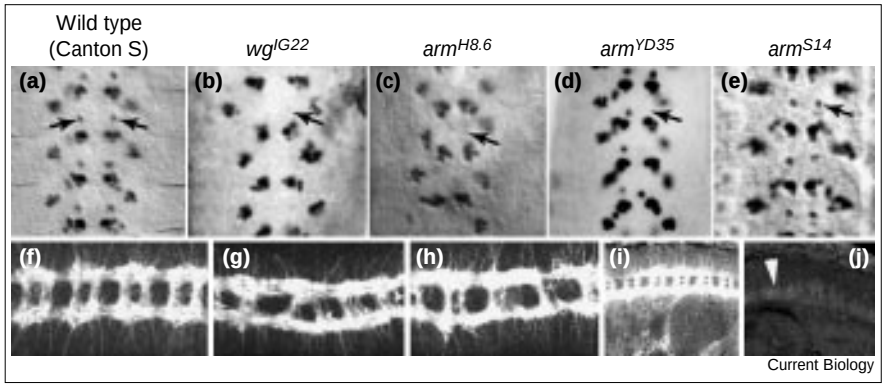

Arm is required for Wg signal transduction during neuroblast fate determination. (a) Wild-type embryos generated two Eve-expressing RP2 motor neurons (arrows) per segment. (b,c) In *wg*^{IG22} (b) and germ-line-clone-derived *arm*$^{H8.6}$ (c) embryos, no RP2 neurons were detected (arrows). (d) Animals that carried the *arm* null allele (*arm*^{YD35}) zygotically but have wild-type maternal Arm generated a partial set of RP2 neurons (arrow indicates a missing RP2 neuron). (e) The *arm*^{S14} allele rescued Wg signaling in the CNS, resulting in a full set of RP2 neurons (arrow). (f) VNC of wild-type stage 15 embryo labeled with BP102. Both *wg* null (g) and *arm*$^{H8.6}$ germ-line-clone-derived (h) embryos had a broad array of CNS defects including gaps in the longitudinals (data not shown) and poorly formed commissures. (i,j) Wild-type (i) and mutant (j) embryos derived from *arm*^{YD35}/ + parents, labeled with anti-Arm(N2) antibody. In wild-type embryos, Arm accumulated at high levels in the VNC. In *arm* zygotic-null embryos, very low levels of maternal Arm persisted during late CNS development (arrowhead).

time of accumulation suggested that the 120 kDa and > 200 kDa proteins were associated with neural Arm, perhaps because they were enriched in the CNS, though they were also likely to be associated with ubiquitous Arm. We found by immunoblotting that the 120 kDa Arm-associated glycoprotein was likely to be a processed form of *Drosophila* N-cadherin (DN-cadherin, Figure 3b), identified by Iwai *et al.* [9]; their work would also suggest that the approximately 200 kDa glycoprotein is another processed form of DN-cadherin.

Neural Arm is tyrosine-phosphorylated

Ubiquitous Arm is phosphorylated on serine/threonine and tyrosine residues [12]. We examined phosphorylation of neural Arm. Phosphorylation of ubiquitous Arm on serine and threonine residues is easily detected because it alters the mobility of Arm on SDS–PAGE. Neural Arm did not display this altered mobility (Figure 3c) and thus we could not determine by simple means whether neural Arm was phosphorylated on serine and threonine residues. We could demonstrate, however, that a fraction of neural Arm was phosphorylated on tyrosine residues (Figure 3c,d). Wild-type embryo extracts contained both the prominent 82 kDa isoform and a slightly more slowly migrating band (Figure 3d). The upper band specifically cross-reacted with anti-phosphotyrosine antibodies (Figure 3d), suggesting that it was a phosphorylated form of neural Arm. Consistent with this possibility, the upper band was present only at later developmental stages (Figure 3c) and was absent in IPs with anti-Arm(CT) antibody (data not shown). Only a small fraction of neural Arm appeared to be tyrosine-phosphorylated.

Arm functions in neuroblast fate determination through its role in Wg signaling

We examined the effects of *arm* mutations on neuroblast fate determination in the CNS. Wg signaling is required for a number of neuroblast fate decisions [2]; these decisions occur before neural Arm begins to accumulate. As in the epidermis, Arm accumulated in the nuclei and cytoplasm of a subset of neuroblasts (Figure 2c); these are likely to be those that receive the Wg signal. To determine whether *arm* mutations affect Wg signaling in the CNS, we utilized the development of neuroblast 4-2 and its granddaughter, the RP2 neuron, which require Wg signaling to adopt correct fates [2]. RP2 expresses the homeodomain protein Even-skipped (Eve). In parallel, we examined Engrailed (En) expression to assess Wg signaling in the epidermis (see Supplementary material, published with this paper on the internet). Chu-Lagraff and Doe [2] found that, in *wg* mutants, Eve-expressing RP2 neurons are missing (Figure 4b); epidermal En stripes also decay. To specifically inactivate Arm function in Wg signaling, we used the $arm^{H8.6}$ allele, which retains Arm function in adherens junctions but lacks Arm function in epidermal Wg signaling [17]. Embryos that were maternally and zygotically

Figure 5

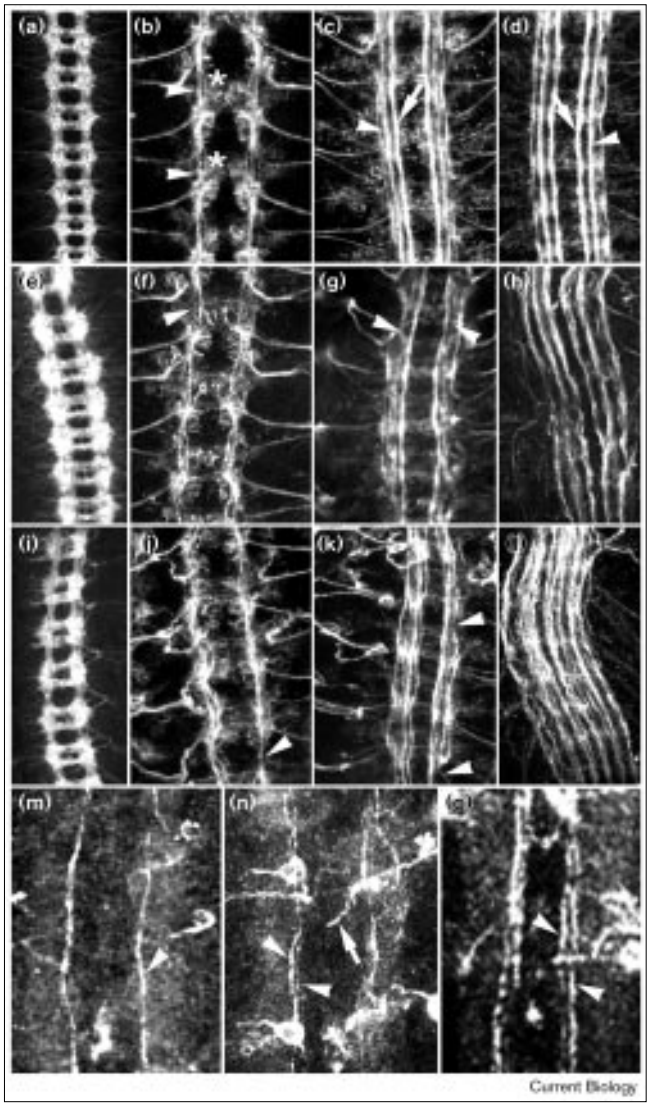

The arm^{S14} and arm^{YD35} mutants have defects in axonal development. (a–d,m) Wild-type, (e–h) arm^{S14} and (i–l,n,o) arm^{YD35} embryos labeled with BP102 antibody (a,e,i), or anti-FasII labeling (b–d,f–h,j–l) or stained for *apterous–tau–lacZ* expression (m–o). (a–d) Wild-type CNS at stage 14 (b), 15 (a,c) and 16 (d). Arrowheads indicate the MP1 pathway, and asterisks in (b) or arrows in (c,d) mark the more medial pCC/MP2 pathway. (e–h) Embryos that were arm^{S14} had an intact VNC with subtle defects. At stage 14 (f), the MP1 fascicle was missing in some segments (arrowhead). By stage 15 (g), prominent gaps in the MP1 pathway were observed (arrowheads). By stage 16 (h), following CNS condensation, FasII-positive axons were loosely associated. (i–l) The arm^{YD35} mutants had similar defects. At stage 14 (j), MP1 was missing in some segments (arrowhead). At stage 15 (k), the MP1 pathway (arrowheads) was disorganized or missing in some segments. (l) Stage 16 axons are loosely associated. (m–o) Expression of *apterous–tau–lacZ* in wild-type (m) and two arm^{YD35} zygotic nulls (n,o). In the wild-type CNS (m), one medial fascicle per longitudinal nerve is labeled (arrowhead). Mutations in *arm* disrupted the integrity of this fascicle (n,o; arrowheads). Occasionally, in abdominal hemisegments, an axon projected towards the midline (n, arrow).

arm$^{H8.6}$ lacked Eve-positive RP2 neurons, consistent with a role for Arm in transduction of the Wg signal in neuroblasts (Figure 4c); epidermal En stripes also decayed (see Supplementary material). We also labeled mutant embryos with the axonal marker BP102, which labels the entire ventral nerve cord (VNC). In both germ-line-clone-derived *arm*$^{H8.6}$, and *wg* embryos, development of the VNC was grossly disrupted (Figure 4g,h), as has been documented by Chu-Lagraff and Doe [2] for *wg*. Doe and colleagues (personal communication) have further analyzed the *arm* phenotype using Huckebein expression to follow cell-fate choices; they have also found that *arm* is required for proper development of neuroblast 4-2.

We also assayed the effects of two other *arm* mutations on Wg signaling in the CNS. Embryos zygotically null for *arm* (*arm*^{YD35}), but which retain wild-type maternal Arm function, had a partial failure of Wg signaling in both the epidermis and CNS (Figure 4d; in these embryos, 70% of the normal number of RP2 neurons were formed). We also examined embryos that were zygotically mutant for *arm*^{S14} (*arm*^{S14} is a mutant transgene that is under the control of the *arm* promoter; *arm*^{S14} 'mutants' are *arm*^{YD35} mutants carrying the transgene). Arm^{S14} protein has a deleted α-catenin-binding site, and thus no longer interacts with α-catenin though it still binds DE-cadherin [5]. Arm^{S14} protein is devoid of adherens junction function [5], but retains full ability to transduce Wg signal in the epidermis [5]. The *arm*^{S14} mutant supported wild-type Wg signaling in the CNS as assayed by development of RP2 neurons (Figure 4e).

Arm functions as a catenin in establishing the proper axonal network

We next examined the consequences for axon outgrowth of removing Arm function. By the time axonogenesis occurred, most wild-type maternal Arm had decayed (Figure 4i,j). We first examined embryos that were zygotically mutant for *arm*^{S14}. In these animals, the catenin function of Arm, but not its Wg signaling role, was selectively disrupted. Animals that were zygotically mutant for *arm*^{S14} develop an intact VNC (Figure 5e), with subtle defects in the development of fasciclin II (FasII)-positive axons (Figure 5f–h), which increased in severity with time. FasII accumulates in a subset of axons within the VNC, which eventually resolves to three fascicles per longitudinal tract, the inner two of which are now referred to as the pCC/MP2 pathway and the MP1 pathway ([18]; Figure 5c,d). Stage 13 *arm*^{S14} mutant embryos were comparable to wild-type embryos in morphology of the overall embryo and FasII-positive neurons (Table 1). Stage 14–16 embryos, however, showed clear, albeit incompletely penetrant, FasII-positive fascicle defects (Table 1), including segmental gaps in the MP1 pathway (arrowhead in Figure 5f). The pCC/MP2 pathway, although typically complete, often undulated less than in wild-type embryos. By stage 15, there were more defects per hemisegment in the MP1 pathway than in the more medial pCC/MP2 pathway (Table 1); these defects included gaps and loss of tight association of fascicles. By stage 16, when CNS condensation is occurring, mature fascicles were more loosely associated in *arm*^{S14} than in wild-type embryos. Very similar defects were seen in *arm*^{YD35} mutants, suggesting that the subtle defects in Wg signaling during neural development seen in this allele did not substantially increase the severity of its VNC phenotype (Figure 5i–l). The indistinguishable phenotypes of *arm*^{YD35} and *arm*^{S14} embryos demonstrated that the defects observed were because of loss of catenin function during axonogenesis, as *arm*^{S14} mutants have full Wg signaling function but lack catenin function [5]. We also used an *apterous–tau–lacZ* reporter [19] which marks a single fascicle in each longitudinal tract. This fascicle was disrupted in *arm*^{YD35} mutant embryos, especially in a condensed CNS (Figure 5, compare (m) and (o)).

Table 1

Axonogenesis defects of *arm* mutants are incompletely penetrant.

	Canton S (wild type) ($n > 109$)	*arm*^{YD35} ($n > 117$)	*arm*^{S14} ($n > 139$)	*arm*^{YD35};*abl*^{1}/*abl*^{4} ($n > 139$)
Stage 13				
MP1	3.4%	5.7%	2.3%	8.0% ($p < 10^{-3}$)
ISN	2.0%	1.4%	0.6%	3.3%
Stage 14				
pCC/MP2	5.1%	4.2%	5.7%	19.1% ($p < 10^{-4}$)
MP1	5.7%	16.9% ($p < 10^{-4}$)	14.6% ($p < 10^{-4}$)	29.0% ($p < 10^{-4}$)
ISN	0.0%	0.8%	0.0%	1.9%
Stage 15				
pCC/MP2	0.6%	7.5% ($p < 10^{-4}$)	2.8% ($p < 10^{-3}$)	37.5% ($p < 10^{-4}$)
MP1	5.4%	21.8% ($p < 10^{-4}$)	21.8% ($p < 10^{-4}$)	53.7% ($p < 10^{-4}$)

The *n* values denote the number of hemisegments examined per embryonic stage, and the ratio of abnormal to normal hemisegments is presented as a percentage. The *p* values were calculated relative to the wild-type control, and are displayed when $p \leq 0.05$. ISN, intersegmental nerve.

Genetic interaction between *arm* and *abl* in the CNS and epidermis

The subtle *arm* phenotype in the CNS suggested two possibilities for Arm's function in axon development. First, Arm may have a more substantial role but this may have been masked phenotypically by the persistence of maternal Arm. Second, the function of Arm during axonogenesis may be redundant with the function of other proteins mediating and/or regulating cell adhesion. We therefore assayed Arm function in a sensitized genetic background, reasoning that a synergistic double-mutant phenotype might identify a gene that either functions with Arm in junctional complex(es) or acts in parallel with those complexes during axonogenesis.

We chose *abl* as a candidate. *The abl* gene encodes a membrane-tethered non-receptor tyrosine kinase localized to regions of cell–cell contact in early epithelia and to axons of the developing CNS [10]. The *abl* mutants survive embryogenesis with few or no CNS defects [20] and die at, or after, pupation [21]. Nevertheless, *abl* mutants have specific axon defects in combination with mutations in other genes, such as *fasI* or *disabled* (*dab*), that individually cause less severe or no embryonic defects (reviewed in [13]). We thus analyzed the nervous systems of *arm;abl* double mutants.

To assess early neural development in *arm;abl* embryos, we examined neural fate determination by assaying expression of Eve, a Wg-dependent marker, and En, which, in the CNS, is Wg-independent. A total of 42 and 160 embryos were examined for Eve and En expression patterns, respectively, which were found to be identical in the arm^{YD35};*abl* double mutants and arm^{YD35} single mutants. We also labeled *arm;abl* embryos with anti-Elav antibody, which marks post-mitotic neurons, and found little gross difference in number of CNS neurons between wild type, *arm* single mutants or *arm;abl* double mutants (Figure 6a–c).

We again analyzed both arm^{YD35} and arm^{S14} mutant animals, to determine whether any effects were due to the role of Arm in Wg signaling or adhesion. Early CNS development was relatively normal in *arm;abl* double mutants. In both arm^{YD35};*abl* and in arm^{S14};*abl* double mutants, however, axonogenesis was dramatically disrupted (Figure 6d–r, Table 2). We examined these defects in detail in arm^{YD35};*abl* double mutants. Disruptions in axon outgrowth were seen as early as stage 14; defects observed included fused or missing commissures (Figure 6r) and segmental gaps along the longitudinal nerves (Figure 6m; arrowheads). During stage 14, we observed increased FasII-staining of axons crossing the midline (Figure 6l; arrows), a phenotype occasionally observed in *arm* mutants but much more penetrant in *arm;abl* double mutants. Defects observed increased in severity as development proceeded, such that, by stage

Figure 6

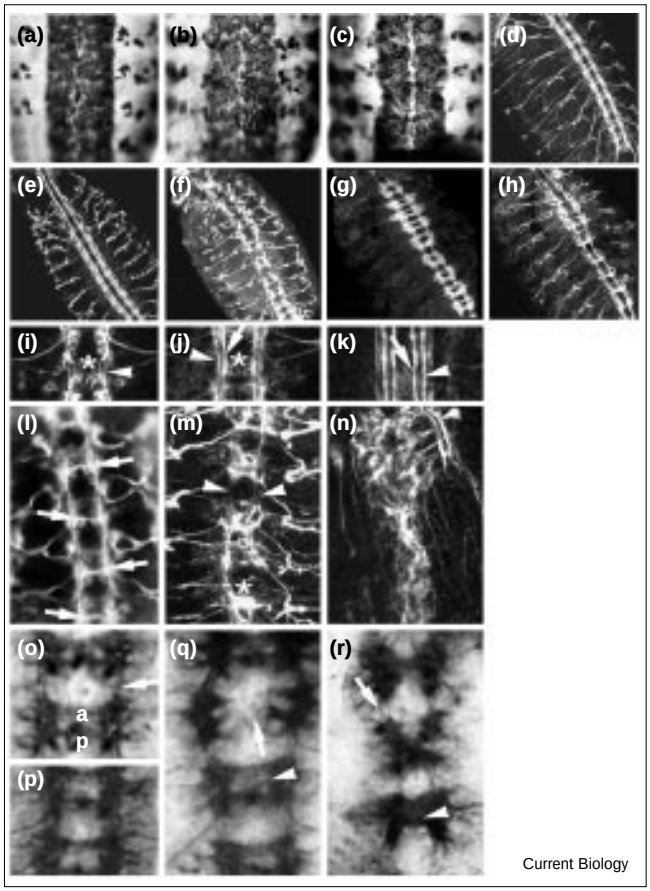

The *arm*;*abl* double mutants have severe defects in axonal development. **(a–c)** Immunostaining with anti-Elav antibody, which labels nuclei of post-mitotic neurons, was similar in the wild-type (a), arm^{YD35} (b) and in a putative arm^{YD35};abl^{1}/*Df(3L)st-j7* embryo (c). Mutants had a disorganized peripheral nervous system. **(d–f)** FasII-positive neurons of stage 15 embryos. Axon morphology was severely disrupted in *arm*;*abl* double mutants (f); compare with wild-type (d) and arm^{YD35} (e) embryos. **(g,h)** The adhesion-defective arm^{S14} transgene did not rescue the *arm;abl* axonogenesis phenotype. In (g), transgene expression was detected using the anti-Arm(CT) antibody. (h) Anti-FasII labeling. **(i–k)** Wild-type embryos labeled with anti-FasII antibody, at stages 14, 15 and 16, respectively (the wild-type pattern is also presented in Figure 5b–d). The *abl* mutant embryos also had a normal CNS (data not shown). The MP1 fascicle (arrowheads) and the pCC/MP2 fascicle (asterisks in i; arrow in j,k) are indicated. **(l–r)** Axonal development in wild-type embryos (o,p) and *arm*;*abl* double mutants (l–n,q,r). All mutants are arm^{YD35};abl^{1}/abl^{4} except (m), which is arm^{XP33};abl^{1}/abl^{1}. In stage 14 *arm;abl* embryos (l), more FasII-positive axons crossed posterior commissures (arrows) than in wild-type embryos. By stage 15 (m), commissural labeling of FasII-positive axons was clearly abnormal (asterisk; compare j with m), and there were prominent gaps in longitudinal nerves (arrowheads). (n) Terminal phenotype. (o–r) BP102 labeling of arm^{YD35}; abl^{1}/ abl^{4} embryos. (o,p) Wild-type VNC. At stage 14 (o), the intersegmental stretches of longitudinal nerves are forming (arrow), as are anterior (A) and posterior (P) commissures. Stage 15 VNCs (p), have a ladder-like structure with complete longitudinal nerves and commissures. In the stage 14 *arm;abl* mutant (q), commissures often failed to form (arrow), or anterior and posterior commissures fused (arrowhead). In the stage 15 *arm;abl* embryo (r), gaps along the longitudinals (arrow) and fused commissures (arrowhead) were seen.

Table 2

The nervous systems of *arm* mutants are sensitive to *abl* mutations.

Genetic cross	Percentage of embryos with normal CNS	Percentage of embryos with *arm*-like CNS	Percentage of embryos with massively disrupted CNS	Number of embryos examined
$abl^1/TM6 \times abl^1/TM6$	98.1	0	1.8	659
$arm^{YD35}/FM7 \times Y/FM7$	72.8	26.2	1.0	191
Prediction for recessive interaction	75.0	18.8	6.2	
$arm^{YD35}/FM7 \times Df(3L)st\text{-}j7/TM6$	67.2	31.1	1.6	305
$arm^{YD35}/+;abl^1/+ \times abl^1/TM6$	75.2	17.9	6.9	1032
$arm^{YD35}/+;abl^1/+ \times Df(3L)st\text{-}j7/TM6$	68.5	23.0	8.5	568
$arm^{YD35}/+;abl^4/+ \times abl^1/+$	70.0	23.1	6.9	290
$arm^{YD35}/+;abl^1, arm^{S14}/+ \times abl^4/TM6$	68.4	23.3	8.3	301
$arm^{YD35}/+;abl^1/+ \times$ *Tn Abl/Tn Abl;Df(3L)std11/TM6*	78.9	20.2	0.8	214

16, the CNS was dramatically disrupted (Figure 6n). We observed defects in other mutant combinations including three *arm* alleles and two *abl* alleles. Furthermore, one copy of wild-type *abl* carried on a transposon significantly reduced the CNS defects of double mutants (Table 2). Heterozygosity for *abl* did not enhance the *arm* CNS defects (Table 2).

Figure 7

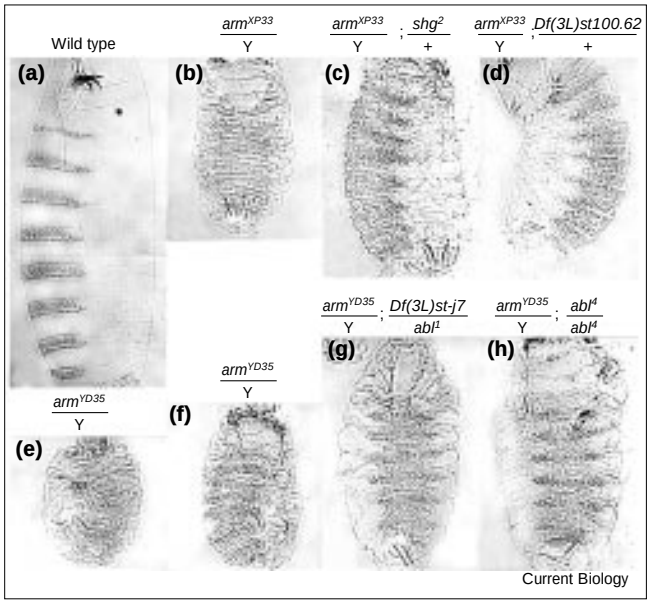

Mutations in the *abl* gene suppress the *arm* segment-polarity phenotype. (a) Wild-type cuticle. Each segment contains anterior denticles; the posterior cuticle is devoid of denticles. (b) A strong *arm* hypomorph; all surviving ventral cells secreted denticles. (c) Reduction of the zygotic DE-cadherin dose by half resulted in suppression of the *arm* segment-polarity phenotype. (d) Removal of one copy of wild-type *abl* resulted in a similar suppression. (e,f) The range of phenotypic severity observed in the zygotic null arm^{YD35}. (g,h) Removal of both copies of *abl* resulted in suppression of the segment-polarity phenotype of the *arm* zygotic null.

As Abl localizes to cell–cell junctions of ectodermal cells, we investigated whether *arm* function in the epidermis was also affected by *abl*. In *arm* mutants, the amount of functional Arm becomes limiting and its dual roles in cell adhesion and in Wg signaling become competitive; most remaining Arm localizes to junctions, however [4]. As a result, a reduction in DE-cadherin dosage suppressed the *arm* segment-polarity phenotype, presumably by liberating junctional Arm to act in signal transduction ([4]; Figure 7c). The *arm* segment-polarity phenotype was also suppressed by mutations in *abl* (Figure 7; detailed data are presented in Supplementary material). This effect was seen in *abl* heterozygotes (Figure 7d) and was further enhanced in *abl* homozygotes (Figure 7g,h). Suppression was seen both using deficiencies that deleted *abl* and in *abl* point mutants. Introduction of a wild-type *abl* transgene reversed the suppression (see Supplementary material).

Discussion

Arm has dual roles in CNS development. Both of the known epithelial functions of Arm — Wg signaling and cadherin-based cell–cell adhesion — are also required in the CNS. Arm functions in Wg signal transduction, directing neuroblast cell-fate decisions. The role of Arm in cell adhesion is required for development of the correct axonal scaffold.

The same Wg signaling pathway is used in epidermal and neural cells

As Wg signaling specifies the fates of certain neuroblasts [2], we investigated whether Arm transduces the Wg signal as it does in the epidermis. Mutations in *arm* that block Wg signaling had phenotypes that were identical to those of *wg* nulls in the CNS, using Eve (Figure 4) and Huckebein (C.Q. Doe, personal communication) as markers of neural cell fates. Thus, Arm transduces the Wg signal both in epithelia and during neuroblast fate determination. Wnt signaling also has a role in CNS development in vertebrates; for example, *Wnt-1* mutants have defects in neural cell-fate determination [22,23].

The asymmetric localization of neural Arm suggests a cytoskeletal role

Both the asymmetric localization in axons of neural Arm and its structure (lacking the normal carboxyl terminus that is important in Wg signaling) suggest that it has a catenin function, regulating adhesion during axon outgrowth. Our hypothesis is that DN-cadherin and neural Arm function together during axonogenesis. DN-cadherin is the predominant classical cadherin accumulating in axons [9]. Mutations in DE-cadherin affect accumulation of ubiquitous Arm but not that of neural Arm [24], whereas DN-cadherin is required for neural Arm stability [9]. We found that neural Arm co-immunoprecipitated with a set of glycoproteins that were distinct from DE-cadherin; at least one of these is likely to be a processed form of DN-cadherin. In parallel work, Iwai *et al.* [9] have provided evidence that two of the other glycoproteins also may be processed forms of DN-cadherin.

Neural Arm lacks the carboxy-terminal domain of ubiquitous Arm that is important for Wg signaling [5]. This suggested that neural Arm might be expressed in the CNS to prevent an inappropriate response to the Wg/Wnt signal. We tested this by replacing neural Arm with ubiquitous Arm in the CNS, using a prespliced transgene. This had no detectable effect on neurogenesis; animals expressing only ubiquitous Arm survived to adulthood and were fertile (Figure 2m and data not shown). Neural Arm could thus be replaced by ubiquitous Arm in the CNS. This observation is not unique to Arm; replacement of the neural splice variant of Dopa decarboxylase with the epidermal form in the fly has no noticeable consequences [25]. Thus, neural Arm may have no special role, or this role may only be revealed by more subtle phenotypic assays.

Arm has an important role in axonogenesis through its catenin function

Selective disruption of the role of Arm in Wg signaling resulted in cell-fate defects in both epithelial and CNS development (Figure 4). In contrast, specific removal of the adhesive catenin function of zygotic *arm* resulted in defects in the axon network (Figure 5). We should not, however, forget what occurs correctly in an *arm* mutant. In arm^{S14} mutants, neuroblasts and neurons appeared to be programmed essentially normally, allowing the embryo to begin axonogenesis with the appropriate players. The earliest stages in axon outgrowth were also relatively normal. Neurons formed axons, axons extended and associated with other axons. The basic axonal scaffold was assembled, suggesting that most axons found their appropriate targets. When we focused on specific subsets of axons in greater detail , however, we saw fine-scale defects in axon outgrowth. These defects were seen in arm^{S14} animals, in which Wg signaling was normal, demonstrating that the defects involved the junctional function of Arm rather than its role in Wg signaling. It is satisfying that the *arm* mutant phenotypes are very similar to those observed in the simultaneous investigation of *DN-cadherin* mutants [9], DN-cadherin being the putative partner of Arm in cell–cell adhesion in neurons. This observation strongly supports a model in which the role of Arm in axon development is a junctional one, and strongly suggests that it acts in axons, which is the only place within the CNS where DN-cadherin is found. Like *DN-cadherin* mutants [9], the *arm* VNC phenotype was incompletely penetrant and variable. We observed gaps in particular fascicles, less well-defined fascicles, and broadened regions of axons; these defects may be attributable to axon stalling, misguidance, failure to fasciculate with pioneer neurons, or a combination of these problems.

Arm and Abl may act together in neurons and at adherens junctions

The *arm;abl* double mutants had a severely disrupted CNS. This genetic interaction involves Arm's catenin function and not its role in Wg signaling. The double-mutant phenotype, although much more severe than that of *arm* alone, shared many qualitative similarities. The *abl* mutation thus enhanced phenotypes seen in *arm* single mutants. Certain axons, however, such as the peripheral motor neurons, retained the ability to grow towards targets in the *arm;abl* double mutants.

Arm and Abl could either be participating in the same biochemical cell-adhesion system (cadherin-based cell–cell adhesion) or functioning in distinct, semi-redundant systems (for example, cadherin-mediated adhesion and Abl–FasI-mediated adhesion). One piece of evidence supports the idea that Arm and Abl act together in adherens junctions. In *arm;abl* double mutants, the segment-polarity phenotype of *arm* was suppressed (Figure 7). Similar suppression results from reducing the gene dosage of a known adherens junction protein, DE-cadherin [4]; we suspect that this suppression occurred by liberating maternally contributed Arm from junctions, making it available for Wg signal transduction. If *abl* mutations disabled a cell-adhesion system distinct from cadherin–catenins, then the Arm pool interacting with cadherin should not be dramatically affected. The simplest explanation of the *abl* suppression is that Abl normally promotes adherens junction assembly; its removal would thus both enhance the effects of *arm* mutations on axonogenesis, which requires the catenin function of Arm, and suppress its signaling defect, as junctions and signaling compete for a limited pool of Arm in an *arm* mutant. Further research is necessary to understand the biochemical basis for these genetic observations. For example, Arm may be a substrate for Abl tyrosine kinase *in vivo*. Axonogenesis is also regulated by tyrosine phosphatases (reviewed in [26]). Several *Drosophila* receptor tyrosine phosphatases are involved in axon pathfinding, and vertebrate receptor tyrosine phosphatases interact with cadherins and catenins; β-catenin itself may be a phosphatase target.

Arm may have additional roles in neural development

We suspect that the axon-outgrowth defects of *arm* mutant animals result from the loss of calcium-dependent adhesion. Nevertheless, the defects could also be due to the inhibition of a juxtacrine or paracrine signal generated by cadherin-mediated adhesion and acting through Arm to maintain fascicles. Conversely, cadherin–catenin complexes may be targets of signals modulating intercellular adhesion and, thus, regulate adhesive plasticity during axon pathfinding, CNS condensation, and synaptic re-organization. One candidate for catenin-based signaling is the epidermal growth factor receptor, which associates with cadherin–catenin complexes, mediating tyrosine phosphorylation of β-catenin [27]. Another signal that Arm might transduce is that of DWnt-3, which accumulates along axons; DWnt-3 overexpression results in CNS defects [28].

Materials and methods

Molecular and genetic experiments

The Canton S wild type was used unless noted. Germ-line clones were generated as in [4]. Cuticles were prepared and embryos staged as in [29]. A *Drosophila* adult head cDNA library [30] was screened with an *arm* probe. Phage inserts were subcloned and screened by PCR using *arm* primers flanking exon 4 (nucleotides 2728–2748 of exon 3, and nucleotides 3750–3770 of exon 5) and primers flanking exon 6 (nucleotides 3865–3885 of exon 5, and 4282–4302 of exon 7). PCR products were subcloned using the TA Cloning kit (Invitrogen). Total RNA was assayed by RT–PCR using the Invitrogen cDNA cycle kit as instructed.

Antibody and protein experiments

Antisera against the carboxy-terminal 43 amino acids of ubiquitous Arm fused to GST were produced in rats by Pocono Rabbit Farms. Details of antibody purification are provided in Supplementary material. The antibody recognizes Arm by immunoblotting at 1:800; no additional bands are seen at 1:40. Immunofluorescence was as in [4] (anti-Arm(CT) antibody at 1:40), using FITC-conjugated and/or rhodamine-conjugated secondary antibodies (Boehringer-Mannheim). Specimens were viewed on a Zeiss laser-scanning confocal microscope. For double-labeled images, data from the two channels were superimposed using LSM 3.8 software, with the FITC channel in green and the rhodamine channel in red. Bandpass filters were set to prevent bleed-through between the fluorophore emissions. Eve and En staining were as in [31]. Embryo extracts were prepared and immunoblotted with mouse monoclonal antibody anti-Arm(7A1) at 1:500 as in [15], purified rat polyclonal antibody anti-Arm(CT) at 1:400, or anti-P-Tyr (Upstate Biotechnology, Inc.) at 1:800. AP-conjugated secondary antibody was used for NBT/BCIP detection. Immunoprecipitations were done as in [15]. Extracts were precipitated with anti-Arm(N2-7A1) at 1:20 or anti-Arm(CT) at 1:10. For con A labeling, biotinylated-con A (Pierce) was used at 10 μg/ml in TBST. The filter was probed with AP-conjugated avidin (Pierce) and incubated with NBT/BCIP (Promega).

Supplementary material

Details on antibody purification, a figure showing Wg-dependent maintenance of En stripes, and three tables showing RP2 neuron counts, hatching rates of *arm* mutants in *abl* mutant backgrounds, and suppression of ventral patterning defects in *arm* mutants by *abl* mutations are presented in Supplementary material published with this paper on the internet.

Acknowledgements

We are extremely grateful to H. Harkins for initiating this project. We thank F. Hoffmann, C. Doe, C. Goodman, the Developmental Studies Hybridoma Bank and J. O'Tousa for reagents; M. Takeichi, T. Uemura, A. Comer, F. Hoffmann, C. Doe and F. Gertler for unpublished data and discussions; J. Shields and C. Brown for lab management; S. Whitfield for photography; and R. Biggs, A. Burke, S. Cain, S. Crews, C. Doe, R. Duronio, F. Gertler, S. Grant, T. Uemura and lab members for comments on the manuscript. This work was supported by NIH GM47857 and the Searle Scholars Program.

References

1. Cavallo R, Rubenstein D, Peifer M: Armadillo and dTCF: a marriage made in the nucleus. *Curr Opin Genet Dev* 1997, 7:459-466.
2. Chu-Lagraff Q, Doe C: Neuroblast specification and formation regulated by ***wingless*** in the ***Drosophila*** CNS. *Science* 1993, 261:1594-1597.
3. Pai L-M, Kirkpatrick C, Blanton J, Oda H, Takeichi M, Peifer M: ***Drosophila*** α-catenin and E-cadherin bind to distinct regions of ***Drosophila*** Armadillo. *J Biol Chem* 1996, 271:32411-32420.
4. Cox RT, Kirkpatrick C, Peifer M: Armadillo is required for adherens junction assembly, cell polarity, and morphogenesis during ***Drosophila*** embryogenesis. *J Cell Biol* 1996, 134:133-148.
5. Orsulic S, Peifer M: An ***in vivo*** structure-function analysis of armadillo, the β-catenin homologue, reveals both separate and overlapping regions of the protein required for cell adhesion and wingless signaling. *J Cell Biol* 1996, 134:1283-1301.
6. Matsunaga M, Hatta K, Nagafuchi A, Takeichi M: Guidance of optic nerve fibres by N-cadherin adhesion molecules. *Nature* 1988, 334:62-64.
7. Riehl R, Johnson K, Bradley R, Grunwald GB, Cornel E, Lilienbaum A, Holt CE: Cadherin function is required for axon outgrowth in retinal ganglion cells ***in vivo***. *Neuron* 1996, 17:837-848.
8. Stone KE, Sakaguchi DS: Perturbation of the developing ***Xenopus*** retinotectal projection following injections of antibodies against β1-integrin receptors and N-cadherin. *Dev Biol* 1996, 180:297-310.
9. Iwai Y, Usui T, Hirano S, Steward R, Takeichi M, Uemura T: Axon patterning requires DN-cadherin, a novel neuronal adhesion receptor, in the ***Drosophila*** embryonic CNS. *Neuron* 1997, 19:77-89.
10. Bennett RL, Hoffmann FM: Increased levels of the ***Drosophila*** Abelson tyrosine kinase in nerves and muscles: subcellular localization and mutant phenotypes imply a role in cell-cell interactions. *Development* 1992, 116:953-966.
11. Takahashi F, Endo S, Kojima T, Saigo K: Regulation of cell-cell contacts in developing ***Drosophila*** eyes by ***Dsrc41***, a new, close relative of vertebrate c-***src***. *Genes Dev* 1996, 10:1645-1656.
12. Peifer M, Pai L-M, Casey M: Phosphorylation of the ***Drosophila*** adherens junction protein Armadillo: roles for Wingless signal and Zeste white-3 kinase. *Dev Biol* 1994, 166:543-556.
13. Hoffmann F: ***Drosophila*** abl and genetic redundancy in signal transduction. *Trends Genet* 1991, 7:351-355.
14. Tepass U, Hartenstein V: The development of cellular junctions in the ***Drosophila*** embryo. *Dev Biol* 1994, 161:563-596.
15. Peifer M: The product of the ***Drosophila*** segment polarity gene ***armadillo*** is part of a multi-protein complex resembling the vertebrate adherens junction. *J Cell Sci* 1993, 105:993-1000.
16. Oda H, Uemura T, Harada Y, Iwai Y, Takeichi M: A ***Drosophila*** homolog of cadherin associated with Armadillo and essential for embryonic cell-cell adhesion. *Dev Biol* 1994, 165:716-726.
17. Peifer M, Sweeton D, Casey M, Wieschaus E: ***wingless*** signal and Zeste-white 3 kinase trigger opposing changes in the intracellular distribution of Armadillo. *Development* 1994, 120:369-380.
18. Hidalgo A, Brand AH: Targeted neuronal ablation: the role of pioneer neurons in guidance and fasciculation in the CNS of ***Drosophila***. *Development* 1997, 124:3253-3262.
19. Lundgren S, Callahan C, Thor S, Thomas J: Control of neuronal pathway selection by the Drosophila LIM homeodomain gene apterous. *Development* 1995, 121:1769-1773.
20. Elkins T, Zinn K, McAllister L, Hoffmann F, Goodman C: Genetic analysis of a ***Drosophila*** neural cell adhesion molecule: Interactions of fasciclin I and Abelson tyrosine kinase mutations. *Cell* 1990, 60:565-575.
21. Gertler F, Bennett R, Clark M, Hoffmann F: Drosophila abl tyrosine kinase in embryonic CNS axons: a role in axonogenesis is revealed through dosage-sensitive interactions with disabled. *Cell* 1989, 58:103-113.
22. McMahon AP, Bradley A: The ***Wnt-1 (int-1)*** proto-oncogene is required for development of a large region of the mouse brain. *Cell* 1990, 62:1073-1085.
23. Thomas KR, Capecchi MR: Targeted disruption of the murine int-1 proto-oncogene resulting in severe abnormalities in midbrain and cerebellar development. *Nature* 1990, 346:847-859.

24. Uemura T, Oda H, Kraut R, Hatashi S, Kataoka Y, Takeichi M: Zygotic DE-cadherin expression is required for the processes of dynamic epithelial cell rearrangement in the ***Drosophila*** embryo. *Genes Dev* 1996, 10:659-671.
25. Morgan BA, Johnson WA, Hirsh J: Regulated splicing produces different forms of dopa decarboxylase in the central nervous system and hypoderm of ***Drosophila melanogaster***. *EMBO J* 1986, 5:3335-3342.
26. Tonks NK, Neel BG: From form to function: signaling by protein tyrosine phosphatases. *Cell* 1996, 87:365-368.
27. Hoschuetzky H, Aberle H, Kemler R: β-catenin mediates the interaction of the cadherin-catenin complex with epidermal growth factor receptor. *J Cell Biol* 1994, 127:1375-1380.
28. Fradkin LG, Noordermeer JN, Nusse R: The ***Drosophila*** Wnt protein DWnt-3 is a secreted glycoprotein localized on the axon tracts of the embryonic CNS. *Dev Biol* 1995, 168:202-213.
29. Wieschaus E, Nüsslein-Volhard C: Looking at embryos. In *Drosophila*, *A Practical Approach*. Edited by Roberts DB. Oxford: IRL Press. 1986:199-228.
30. Itoh N, Salvaterra P, Itakura K: Construction of an adult head cDNA expression library with lambda gt11. *Drosophila Information Newsletter* 1985, 61:89.
31. Patel NH, Snow PM, Goodman CS: Characterization and cloning of fasciclin III: a glycoprotein expressed on a subset of neurons and axon pathways in ***Drosophila***. *Cell* 1987, 48:975-988.

Because *Current Biology* operates a 'Continuous Publication System' for Research Papers, this paper has been published on the internet before being printed. The paper can be accessed from http://biomednet.com/cbiology/cub – for further information, see the explanation on the contents page.

Supplementary material

Roles of Armadillo, a *Drosophila* catenin, during central nervous system development

Joseph Loureiro and Mark Peifer

Current Biology 1998, 8:622–632
http://biomednet.com/elecref/0960982200800622

Figure S1

Wg-dependent maintenance of En stripes. (a) In wild-type embryos, En accumulated in the posterior compartment of germband-retracted embryos. (b,c) En expression was not maintained in *wg* null (b) and germ-line-clone-derived $arm^{H8.6}$ (c) embryos. (d) En expression was partially maintained in an *arm* zygotic null. (e) Zygotic arm^{S14} fully maintained En expression in the epidermis.

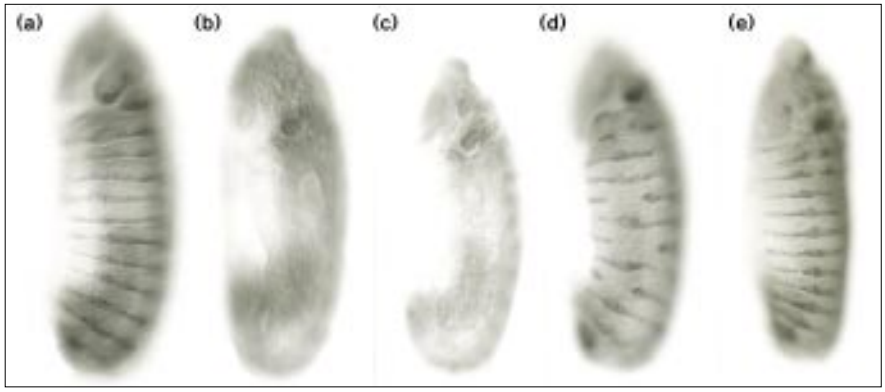

Table S1

RP2 neuron development requires *arm*.

Genotype	Number of RP2 neurons per segment	Number of embryos examined
Canton S (wild type)	2 ± 0	41
wg^{lG22}/wg^{lG22}	0 ± 0	63
$arm^{H8.6}$ germ-line clones	0 ± 0	66
arm^{YD35}/Y	1.4 ± 0.2	54
arm^{YD35}/Y;arm^{S14}/+	2.0 ± 0	62
arm^{YD35}/Y;abl^{1}/abl^{4}	1.5 ± 0.3	42

Table S3

Ventral patterning defects in *arm* mutants are suppressed by *abl* mutations.

Genetic cross	*YD35* strong	*YD35* weak	*wg* defects suppressed	Number of embryos
$arm^{YD35}/FM7 \times Y/FM7$	75.6%	20.9%	3.5%	513
$arm^{YD35}/FM7 \times Y/FM7;+/TM6$	77.9%	17.4%	4.7%	317
$arm^{YD35}/FM7 \times Df(3L)st\text{-}j7/TM6$	9.3%	42.9%	47.9%	280
$arm^{YD35}/FM7 \times abl^{1}/TM6$	46.0%	42.2%	11.8%	424
$arm^{YD35}/+;abl^{1}/+ \times abl^{1}/TM6$	27.9%	47.6%	24.5%	926
$arm^{YD35}/+;abl^{4}/+ \times abl^{4}/TM6$	35.5%	51.7%	12.9%	739
$arm^{YD35}/+;abl^{1}/+ \times$ *Tn Abl/Tn Abl;Df(3L)std11/TM6*	50.4%	45.6%	4.0%	526

Table S2

Hatching rates of *arm* mutants do not decrease in *abl* mutant backgrounds.

Genetic cross	Hatching rate	Number of embryos examined
$abl^{4}/+ \times abl^{1}/TM6$	90.7%	385
$+/Y \times arm^{YD35}/FM7$	73.5%	473
$+/Y;abl^{1}/TM6 \times arm^{YD35}/FM7$	73.0%	474
$+/Y;abl^{1}/TM6 \times arm^{YD35}/+;abl^{4}/+$	77.0%	267

Materials and methods

Production and purification of rat anti-Arm(CT) antibody

Antisera were produced by Pocono Rabbit Farms, following their standard protocol. Briefly, rats were injected with a bacterially produced fusion protein carrying the carboxy-terminal-most 43 amino acids of full-length Armadillo fused to GST. Rat serum (250 µl) was diluted 1:3 in PBS/0.1% BSA/0.02% sodium azide, and anti-Arm(CT) Ig was purified from it by incubating it for 2 h at room temperature with reusable strips of nitrocellulose carrying the immunizing fusion protein immobilized onto them. The nitrocellulose strips had been preblocked for 1 h at room temperature in PBS/5% BSA. Following incubation with serum, the unbound fraction was removed and the strips were washed with PBS/0.1% BSA. Bound antibody was eluted by incubating strips with 500 µl elution buffer (3M glycine pH 2.5) for 20 min at room temperature. The eluate was transferred to a microfuge tube and neutralized with 0.1 volume 1 M Tris base pH 8.0, and 0.1 volume 10 × PBS/0.02% sodium azide was added. Ig was stored at 4°C, or 0.2 volume glycerol was added for storage at –80°C. The eluted fraction recognizes the 105–115 kDa Armadillo isoforms at 1:800, and at a dilutions of 1:40 still recognize only these Armadillo isoforms and no other proteins. Immunolocalization was done at 1:40.